




Biosynthesis and Characterization of Iron Nanoparticles Using *Pseudomonas* and Actinobacteria

S. Nazma¹, T. Sudha², D. P. Biradar¹, P. U. Krishnaraj³, S. S. Chandrashekhara⁴ and H. Ravikumar⁵

¹Dept. of Agronomy, ²Dept. of Agronomy, ³Dept. of Agricultural Microbiology, ⁴Dept. of Seed Science and Technology, ⁵Dept. of Biotechnology, College of Agriculture, University of Agricultural Sciences, Dharwad, Karnataka (580 005), India



Corresponding  nazmashaik095@gmail.com

 0009-0009-0679-5442

ABSTRACT

The experiment was carried out during 2022 to study on the biosynthesis and characterization of iron nanoparticles in the Green Nanotechnology Laboratory, University of Agricultural Sciences, Dharwad, Karnataka, India. Collection and screening of *Pseudomonas* and actinobacterial isolates were done at the Microbial Genetics Laboratory, Department of Agricultural Microbiology of the university and the iron nanoparticles were biosynthesized and characterized through UV-Visible spectroscopy, Particle Size Analyzer (PSA), Scanning Electron Microscope (SEM), (EDX), X-ray diffraction (XRD) and Fourier Transform Infrared Spectroscopy (FTIR). The formation of the FeNPs was preliminary confirmed by the change in the colour of the reactant mixture visually by monitoring the change in colour from orange to black colour. The iron nanoparticles (FeNPs) synthesized through AUDP209 (*Pseudomonas*) and AUDT636 (actinobacteria) exhibited peak values at 294 and 297 nm, with average sizes of 51.7, and 58.0 nm, respectively. SEM images revealed the spherical shape of the biosynthesized iron nanoparticles (FeNPs), while EDX confirmed the iron ions presence in the biosynthesized samples and the crystalline structure of the iron nanoparticles was confirmed by XRD. FeNPs biosynthesized through AUDP209 showed the absorption peaks at 2337 cm⁻¹, 1639 cm⁻¹, 1118 cm⁻¹, 794 cm⁻¹, 540 cm⁻¹ and FeNPs biosynthesized through AUDT636 showed the absorption peaks at 3741 cm⁻¹, 2349 cm⁻¹, 2067 cm⁻¹, 964 cm⁻¹, 551 cm⁻¹. FTIR spectroscopy confirmed the organic compounds present in the microbial extracts responsible for the capping and stabilizing agents for biosynthesis of FeNPs.

KEYWORDS: Biosynthesis, iron, nanoparticles, nanotechnology

Citation (VANCOUVER): Nazma et al., Biosynthesis and Characterization of Iron Nanoparticles Using *Pseudomonas* and Actinobacteria. *International Journal of Bio-resource and Stress Management*, 2025; 16(4), 01-07. [HTTPS://DOI.ORG/10.23910/1.2025.5736](https://doi.org/10.23910/1.2025.5736).

Copyright: © 2025 Nazma et al. This is an open access article distributed under the terms of the Creative Commons Attribution-NonCommercial-ShareAlike 4.0 International License, that permits unrestricted use, distribution and reproduction in any medium after the author(s) and source are credited.

Data Availability Statement: Legal restrictions are imposed on the public sharing of raw data. However, authors have full right to transfer or share the data in raw form upon request subject to either meeting the conditions of the original consents and the original research study. Further, access of data needs to meet whether the user complies with the ethical and legal obligations as data controllers to allow for secondary use of the data outside of the original study.

Conflict of interests: The authors have declared that no conflict of interest exists.

1. INTRODUCTION

Nanotechnology may help bring about a new technological revolution in agriculture. Several problems with conventional biofortification could potentially be resolved by nanotechnology (Shakiba et al., 2020). It is possible to produce nanofertilizers using nanomaterials because of their high surface-to-volume ratio, gradual and controlled release at target places, and other characteristics (Feregrino-Perez et al., 2018). The encapsulation of nutrients with nanomaterials results in efficient nutrient absorption by plants, due to the gradual or controlled release of nanoparticles and simple passage through biological barriers by nanoparticles entering the plant vascular system (Solanki et al., 2015; Zulfiqar et al., 2019 and De La Torre-Roche et al., 2020). In comparison to conventional fertilizers, long-term delivery of plants via nanofertilizers enables enhanced crop growth. As nanofertilizers are added in small amounts, these also prevent soil from becoming burdened with the by-products of chemical fertilizers and reduce the environmental hazards (Silva et al., 2018). Unlike chemical fertilizers, nanofertilizers can be synthesized and applied based on the crop's nutritional needs and the status of the soil's nutrient levels using biosensors (Kah et al., 2018). Additionally, nanofertilizers, as opposed to chemical fertilizers, allow for high mineral bioavailability to plants due to their smaller size, greater reactivity, and higher surface area (Liu and Lal, 2015).

Iron (Fe), an essential nutrient for the crop growth and development of crops. It is essential for the formation of chlorophyll and is involved in the electron transport system and activation of several enzymatic functions (Elemike et al., 2019 and Chugh et al., 2022). Chlorosis in young plant leaves is the main sign of Fe deficiency, which affects both physiological function and nutritional quality (Kasote et al., 2019 and Ali et al., 2021). Fe absorption by plants is frequently limited because ferric oxide (Fe_2O_3), also known as hematite, is the most prevalent form of Fe and is highly insoluble in soils. In the food chain, Fe shortage affects not only plant growth and development but also causes Fe insufficiency in both animals and humans. Therefore, it's critical to increase the effectiveness of Fe fertiliser use (Rout and Sahoo, 2015 and Dhage and Vidyashree, 2022).

Synthesis of nanoparticles involves a variety of biological, physical and chemical methods. Among which, microbial synthesis of metal oxide nanoparticles has received enormous attention due to the advances in cost effectiveness, environmental friendly. (Saravanan et al., 2021 and Abid et al., 2022). Traditional chemical methods, which could be hazardous to the environment, are being replaced with biological systems, which are preferred for NP synthesis (Busi and Rajkumari, 2019; Rana et al., 2020 and Bogas et al.,

2022). For synthesis of nanoparticles, many microorganisms have been used, including bacteria, actinobacteria, fungus, yeast, and algae (Dhanker et al., 2021 and Alsaiani et al., 2023). Microorganisms (fungi, viruses, bacteria, yeast, and actinomycetes) can be thought of as biological nanofactories since they can take in metal ions from the environment and change them into elemental compounds. These processes can take place as either intracellular or extracellular events, and as a result, NPs produced by bacteria are categorized as either intracellular or extracellular NPs (Koc and Karayigit, 2022). Microbial pathways do not produce any toxic by-products and chemicals during the nanoparticles synthesis, it has been proposed as feasible alternatives to physico-chemical methods. Additionally, bacteria are great producers of NPs it they can create a variety of secondary metabolites (Ovais et al., 2018; Fadiji and Babalola, 2020 and Rani et al., 2022). Keeping the above facts in view, the present investigation was planned to study on the biosynthesis of iron nanoparticles using two different microbial strains and characterized through UV-Vis Spectroscopy, PSA, SEM, EDX, XRD and FTIR.

2. MATERIALS AND METHODS

2.1. Biosynthesis of iron nanoparticles

The *Pseudomonas* and actinobacterial isolates were collected from culture collection maintained at Microbial Genetics Laboratory, Department of Microbiology, UAS, Dharwad, during 2022. The collected isolates were spotted and sub cultured in King's B and Starch casein agar media (pH 7) and incubated for 2 and 7 days, respectively, in incubator at 30°C.

2.1.1. Biosynthesis of iron nanoparticles using *Pseudomonas* strain AUDP209 and

2.1.2. Actinobacterial strain AUDT636

Bacterial cells were inoculated into each of Erlenmeyer flasks containing 100 mL of the King's B and Starch casein broth and placed in a shaker incubator at 30°C and 150 rpm for two and seven days to grow, respectively. After the incubation time, the pH of the culture broth was adjusted to 10–11 using 1% NaOH. At the end of each incubation period, the liquid medium was centrifuged at 10,000 rpm for 15 min to remove cell debris. Then, 100 mM ferrous sulphate hepta hydrate was added to the supernatant solution and heated in a water bath in the range of 80°C for 10 min. The flasks were taken out from the water bath and kept in a shaker incubator at 150 rpm for 24 h at 30°C until all particles settled down at the bottom of the flask, further sonication was done for 30 minutes. The pellet was then collected by centrifugation at 10,000 rpm for 5 minutes and washed with deionized water three times followed by drying at 40°C for 48 h in a hot air oven and dried powder

was used for characterization.

2.2. Characterization of biosynthesized iron nanoparticles

2.2.1. UV-Visible spectroscopy

The confirmation of nanoparticle reduction was achieved through UV-Visible spectrophotometer analysis at scanning wavelengths ranging from 200 to 700 nm, based on their optical absorbance peak. As the nanoparticles' size decreases, the band gap increases, leading to an elevation in optical absorbance compared to bulk particles. Consequently, their colour change. The biosynthesized FeNPs initial sonication was using a solid probe ultrasonicator to ensure a uniform distribution of nanoparticles. Subsequently, the solution was diluted five times with deionized distilled water before spectrophotometric measurement, and an aliquot of the extract served as the control, with absorbance maxima recorded at room temperature.

2.2.2. Particle size analyzer

The average particle size of the NPs was measured using dynamic light scattering (DLS) in a high-performance particle-size analyzer. Before analysis, the sample was diluted and placed in disposable polystyrene cuvettes. The measurements were conducted at room temperature in triplicate, with a scattering angle of 90°.

2.2.3. Scanning electron microscope

The surface morphology of the iron nanoparticles was analyzed through scanning electron microscopy (SEM). The nanoparticles were affixed to an aluminum holder using carbon adhesive tape, and SEM images were captured using an EVO 18 microscope equipped with smart SEM software. Additionally, the presence of iron ions was confirmed through energy-dispersive X-ray spectroscopy (EDS), which was attached to the EVO 18 scanning electron microscope. To examine the pellets obtained through centrifugation of the synthesized nanoparticles, the powder was evenly placed on an aluminum stub, coated with gold in a sputter coater, and observed using SEM at various voltages. The SEM was operated at a working distance of 8-9 mm and a voltage range of 5-10 kV.

2.2.4. X-ray diffraction

The FeNPs powder, after reduction, was exposed to X-ray diffraction (XRD) analysis to examine its crystalline structure. The Rigaku TTR was employed for this purpose, operating at 40 KV and 150 mA, with a 2h scanning range between 10 and 90 degrees using the Cu K α line (wavelength = 0.15406 nm). Furthermore, the particle sizes were determined using the Debye-Scherrer equation.

$$D = k\lambda / \beta \cos\theta$$

Where,

D=Average size of nano particles

k=Scherrer constant, (value 0.9)

λ =The wavelength of radiation (0.15406 nm)

β =Full width half maximum in radians (FWHM)

θ =Angle of diffraction

2.2.5. Fourier transform infrared spectroscopy

The biosynthesized iron nanoparticles powder was utilized for FTIR analysis using an FTIR spectrometer. To identify the existing functional groups in the samples, 25 mg of the particles were briefly dissolved and coated with KBr pellets. The Bruker TENSOR 27 spectrometer was used for this analysis, with a measuring wavelength ranging from 4000 to 400 cm⁻¹ at a resolution of 4 cm⁻¹. The identified bands were then compared with the standard FTIR spectrum to characterize the functional components.

3. RESULTS AND DISCUSSION

3.1. Biosynthesis of iron nanoparticles using microbial extracts

3.1.1. Biosynthesis of FeNPs by using microbial extract of *Pseudomonas* strain AUDP209

After mixing 80 ml of ferrous sulphate heptahydrate with 20 mL of AUDP209 extract for 48 hours in a rotary shaker, microwave irradiation for the 60s, and ultrasonication for 30 minutes, the formation of FeNPs was observed. The reduction was confirmed visually by monitoring the change in colour from orange to dark green (Figure 1). These results were in conformity with Khan et al., 2021 and Desai and Pawar, 2020, who used *Pseudomonas* bacteria extracts to biosynthesize FeNPs.



Figure 1: Biosynthesis of iron nanoparticles using *Pseudomonas* strain AUDP209

3.1.2. Biosynthesis of FeNPs by using microbial extract of actinobacterial strain AUDT636

After 72 hours of shaking in a rotary shaker with 45 ml of ferrous sulphate heptahydrate mixed with 15 ml of AUDT636 extract, the synthesis of FeNPs was observed. This was then followed by microwave irradiation for 60s and ultrasonication for 30 minutes. The reduction was confirmed visually by monitoring the change in colour from orange

to black from *Streptomyces* spp (Figure 2) as reported by Rajeswaran et al., 2020.



Figure 2: Biosynthesis of iron nanoparticles using actinobacteria strain AUDT636

3.2. Characterization of biosynthesized iron nanoparticles

3.2.1. UV-Visible spectroscopy

The UV-visible spectrophotometer, which uses surface plasmon resonance to identify the maximum peak, is an efficient preliminary test to confirm the formation of nanoparticles (NPs). Maximum peaks for FeNPs biosynthesized through AUDP209 and AUDT636 were observed at wavelengths of 294 and 297 nm, respectively (Figure 3a and b). Similar findings were reported by Crespo et al. (2017), using UV-vis spectroscopy to characterize iron nanoparticles synthesized by *P. aeruginosa*, the highest peak of the surface plasmon resonance was observed at 275 nm.

3.2.2. Particle size analyser

Particle size analyser works on the principle of dynamic light scattering (DLS). The dynamic light scattering method is a non-intrusive method for determining the size and distribution of nanoparticles dispersed in liquid. The DLS method was used to measure the hydrodynamic diameter-based time-dependent oscillation of scattered light in dispersed nanoparticles caused by Brownian motion (Danaei et al., 2018). FeNPs nanoparticles biosynthesized by AUDP209 and AUDT636, the DLS analysis revealed a mean diameter of 51.7 and 58.0 nm, respectively (Figure 4a and b). The results were confirmed by the findings of Crespo et al. (2017), synthesised 23.0 nm FeNPs using *P. aeruginosa*. The average diameter of iron nanoparticles synthesized by *Pseudomonas aeruginosa* was 40.0 nm (Khan et al., 2021).

3.2.3. Scanning electron microscope

The surface morphology of nanoparticles is determined using a scanning electron microscope, and the elemental composition of the NPs was also determined using energy dispersive X-Ray Spectroscopy. FeNPs were biosynthesized from AUDP209 and AUDT636 and were characterized using SEM and EDX. Both biosynthesized samples had spherical shapes (Figure 5a and b), and EDX analysis

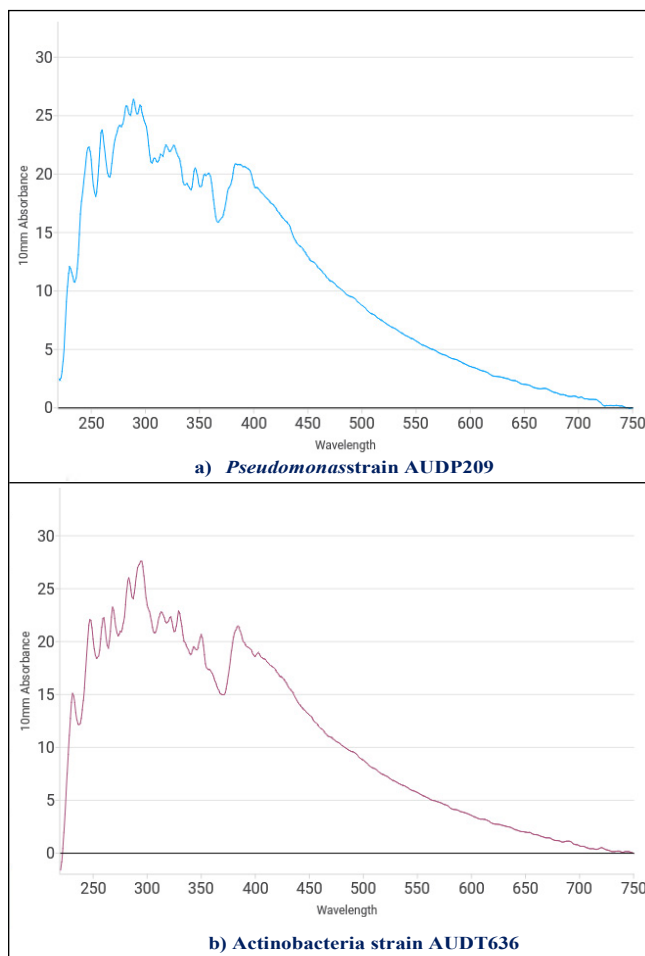


Figure 3: Characterization of biosynthesized iron nanoparticles from *Pseudomonas* strain AUDP209 and actinobacteria strain AUDT636 by UV- Visible spectrophotometer

revealed that the elemental weight percentage of iron was 63.58% and 58.90%, respectively (Figure 6a and b) while the elemental weight percentage of oxygen was 27.78% and 33.57%, respectively. According to Rajeswaran et al. (2020), iron nanoparticles synthesized by *Streptomyces* spp. have a quasi-spherical form. SEM was used to analyze the morphological characteristics of the nanoparticles.

3.2.4. X-ray diffraction

By using XRD, the crystalline nature of the synthesized FeNPs was examined. The peaks in the FeNPs synthesized by AUDP209 and AUDT636 were amorphous in nature. FeNPs synthesized using AUDP209 the peaks were observed at 30.10°, 35.52°, 48.45°, 57.17° and 62.85° which corresponds to (220), (311), (422), (511) and (440), respectively (Figure 7a). Likewise, FeNPs biosynthesized using microbial extract of AUDT636 showed peaks at 28.76°, 35.50°, 43.44°, 48.53°, 57.15° and 62.70° which corresponds to (220), (311), (400), (422), (511) and (440), respectively (Figure 7b). The results were confirmed by

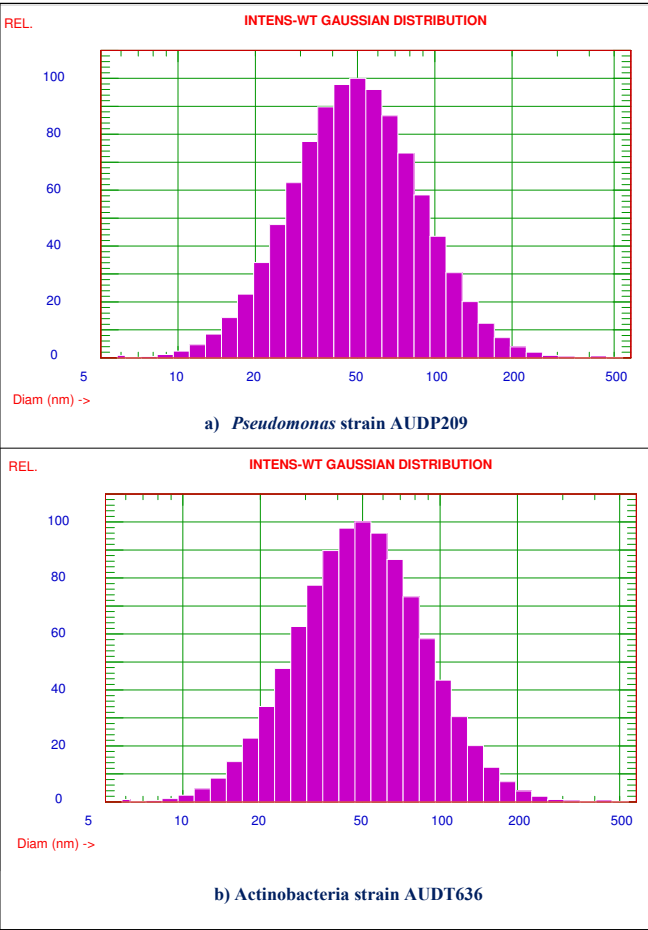


Figure 4: Characterization of biosynthesized iron nanoparticles from *Pseudomonas* strain AUDP209 and actinobacteria strain AUDT636 by particle size analyzer

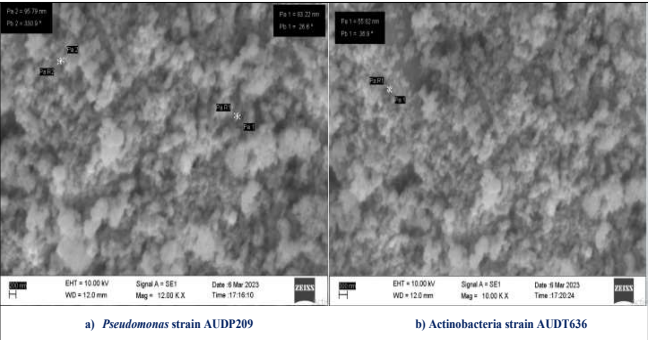


Figure 5: Characterization of biosynthesized iron nanoparticles from *Pseudomonas* strain AUDP209 and actinobacteria strain AUDT636 by scanning electron microscope

the findings of Desai and Pawar (2020), the XRD analysis showed crystalline structure for FeNPs biosynthesized from *Pseudomonas stutzeri* and diffraction patterns at 2θ values of 35.68, 43.36, 53.82, 57.36 and 63.07 which represented [311] [400] [422] [511] and [440] planes respectively.

3.2.5. Fourier transform infrared spectroscopy

The bioactive molecules responsible for the reduction of

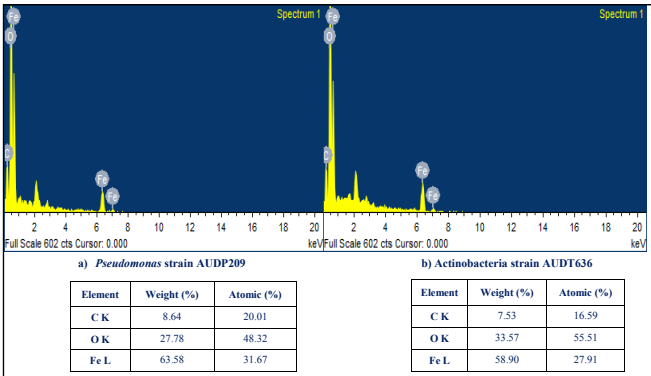


Figure 6: Characterization of biosynthesized iron nanoparticles from *Pseudomonas* strain AUDP209 and actinobacteria strain AUDT636 by energy-dispersive X-ray spectroscopy

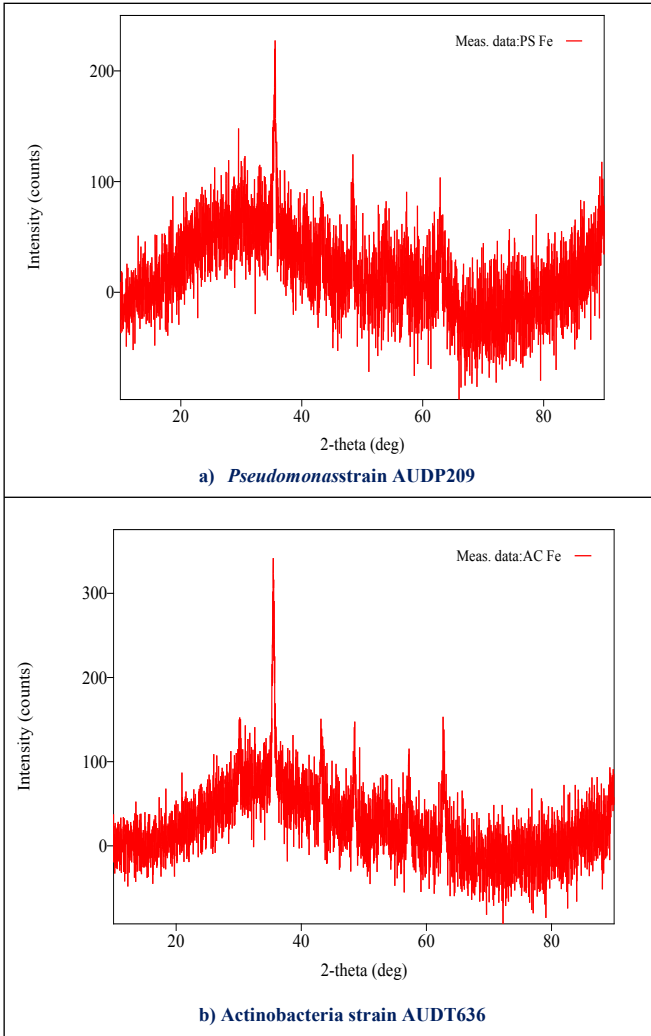


Figure 7: Characterization of biosynthesized iron nanoparticles from *Pseudomonas* strain AUDP209 and actinobacteria strain AUDT636 by X-ray diffraction

Fe ions and the functional groups present in the material were identified and confirmed by fourier-transform infrared spectroscopy. FeNPs synthesized from AUDP209 observed

the highest peaks at 2337 cm^{-1} , 1639 cm^{-1} , 1118 cm^{-1} , 794 cm^{-1} , 540 cm^{-1} (Figure 8a) and FeNPs synthesized from AUDT636 strain showed the highest peaks at 3741 cm^{-1} , 2349 cm^{-1} , 2067 cm^{-1} , 964 cm^{-1} , 551 cm^{-1} (Figure 8b). The FTIR spectrum peak at 675.09 cm^{-1} implied alkenes with C=H stretch. In FTIR spectrum peak shown at 895 cm^{-1} might correspond to stretching S=O of sulfoxide and bending C=C of alkene (Abdo et al., 2021). In the range of $1100\text{--}1200\text{ cm}^{-1}$, there is an area of C-C stretching: C-H and N-H bending vibrations are typical for amide III (Mohamed and Mohammed, 2013).

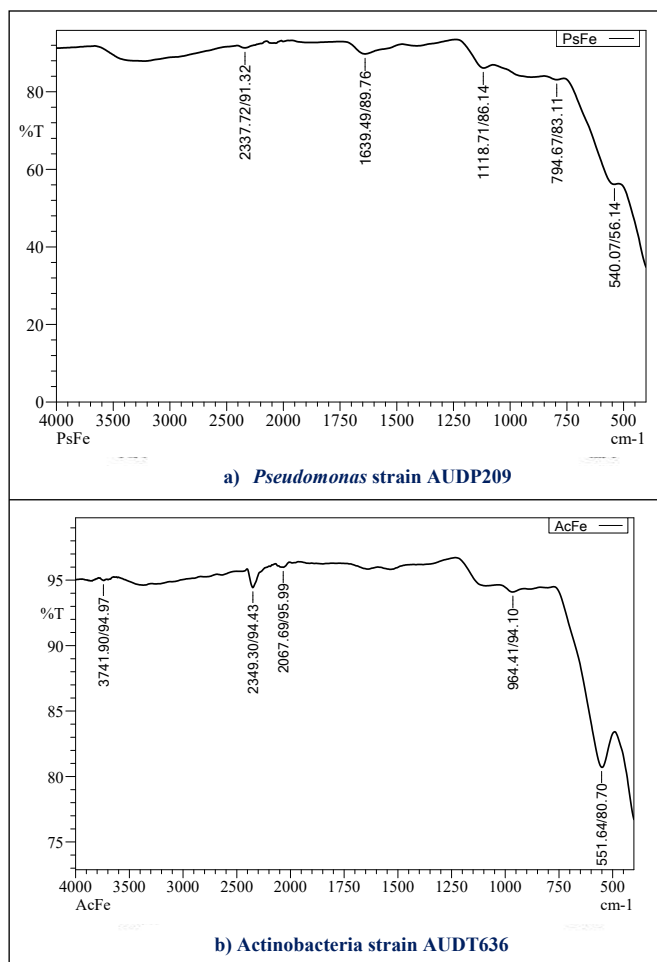


Figure 8: Characterization of biosynthesized iron nanoparticles from *Pseudomonas* strain AUDP209 and actinobacteria strain AUDT636 by fourier transform infrared spectroscopy

4. CONCLUSION

The organic compounds present in the microbial extracts of actinobacteria and *Pseudomonas* acted as both capping and stabilizing agents for the synthesis of ironnanoparticles. The formation of the FeNPs was preliminary confirmed by the change in the colour of the reactant mixture, later the synthesized samples were characterized through UV-Visible Spectroscopy, PSA, SEM, XRD and FTIR Spectroscopy,

where the FeNPs biosynthesized through *Pseudomonas* strain AUDP209 and actinobacteria strain AUDT636.

5. REFERENCES

- Abdo, A.M., Fouda, A., Eid, A.M., Fahmy, N.M., Elsayed, A.M., Khalil, A.M.A., Alzahrani, O.M., Ahmed, A.F., Soliman, A.M., 2021. Green synthesis of Zinc Oxide Nanoparticles (ZnO-NPs) by *Pseudomonas aeruginosa* and their activity against pathogenic microbes and common house mosquito, *Culex pipiens*. Materials 14(22), 6983.
- Abid, N., Khan, A.M., Shujait, S., Chaudhary, K., Ikram, M., Imran, M., Haider, J., Khan, M., Khan, Q., Maqbool, M., 2022. Synthesis of nanomaterials using various top-down and bottom-up approaches, influencing factors, advantages, and disadvantages: A review. Advances in Colloid and Interface Science 300, 102597.
- Alsaiani, N.S., Alzahrani, F.M., Amari, A., Osman, H., Harharah, H.N., Elboughdiri, N., Tahoona, M.A., 2023. Plant and microbial approaches as green methods for the synthesis of nanomaterials: synthesis, applications, and future perspectives. Molecules 28(1), 463.
- Bogas, A.C., Henrique Rodrigues, S., Gonçalves, M.O., De Assis, M., Longo, E., Paiva De Sousa, C., 2022. Endophytic microorganisms from the tropics as biofactories for the synthesis of metal-based nanoparticles: Healthcare applications. Frontiers in Nanotechnology 4(1), 823–836.
- Chugh, G., Siddique, K.H., Solaiman, Z.M., 2022. Iron fortification of food crops through nanofertilisation. Crop and Pasture Science 73(7–8), 736–748.
- Crespo, K.A., Baronetti, J.L., Quinteros, M.A., Paez, P.L., Paraje, M.G., 2017. Intra- and extracellular biosynthesis and characterization of iron nanoparticles from prokaryotic microorganisms with anticoagulant activity. Pharmaceutical Research 34(1), 591–598.
- Danaei, M.R.M.M., Dehghankhold, M., Ataei, S., Hasanzadeh Davarani, F., Javanmard, R., Dokhani, A., Khorasani, S., Mozafari, M.R., 2018. Impact of particle size and polydispersity index on the clinical applications of lipidicnanocarrier systems. Pharmaceutics 10(2), 57–74.
- De La Torre-Roche, R., Cantu, J., Tamez, C., Zuverza-Mena, N., Hamdi, H., Adisa, I.O., Elmer, W., Gardea-Torresdey, J., White, J.C., 2020. Seed biofortification by engineered nanomaterials: a pathway to alleviate malnutrition?. Journal of Agricultural and Food Chemistry 68(44), 12189–202.
- Desai, M.P., Pawar, K.D., 2020. Immobilization of cellulase on iron tolerant *Pseudomonas stutzeri* biosynthesized

- photocatalytically active magnetic nanoparticles for increased thermal stability. *Materials Science and Engineering* 106(1), 110169–181.
- Dhanker, R., Hussain, T., Tyagi, P., Singh, K.J., Kamble, S.S., 2021. The emerging trend of bio-engineering approaches for microbial nanomaterial synthesis and its applications. *Frontiers in Microbiology* 12(1), 638003–29.
- Elemike, E.E., Uzoh, I.M., Onwudiwe, D.C., Babalola, O.O., 2019, The role of nanotechnology in the fortification of plant nutrients and improvement of crop production. *Applied Sciences* 9(3), 499–531.
- Feregrino-Perez, A.A., Magana-Lopez, E., Guzman, C., Esquivel, K., 2018. A general overview of the benefits and possible negative effects of the nanotechnology in horticulture. *Scientia Horticulturae* 238(1), 126–137.
- Kah, M., Kookana, R.S., Gogos, A., Bucheli, T.D., 2018. A critical evaluation of nanopesticides and nanofertilizers against their conventional analogues. *Nature Nanotechnology* 13(1), 677–684.
- Khan, A.A., Khan, S., Khan, S., Rentschler, S., Laufer, S., Deigner, H.P., 2021. Biosynthesis of iron oxide magnetic nanoparticles using clinically isolated *Pseudomonas aeruginosa*. *Scientific Reports* 11(1), 20503.
- Koc, E., Karayigit, B., 2022. Assessment of biofortification approaches used to improve micronutrient-dense plants that are a sustainable solution to combat hidden hunger. *Journal of Soil Science and Plant Nutrition* 22(1), 475–500.
- Liu, R., Lal, R., 2015. Potentials of engineered nanoparticles as fertilizers for increasing agronomic productions. *Science of the Total Environment* 514(1), 131–139.
- Leon-Silva, S., Arrieta-Cortes, R., Fernandez-Luqueno, F., Lopez-Valdez, F., 2018. Design and production of nanofertilizers. *Agricultural nanobiotechnology: modern agriculture for a sustainable future*. Springer International Publishing: Cham, Switzerland, 17–31.
- Rajeswaran, S., Thirugnanasambandan, S.S., Dewangan, N.K., Moorthy, R.K., Kandasamy, S., Vilwanathan, R., 2020. Multifarious pharmacological applications of green routed eco-friendly iron nanoparticles synthesized by *Streptomyces* Sp. (SRT12). *Biological Trace Element Research* 194(1), 273–283.
- Rani, S., Kumar, P., Dahiya, P., Dang, A.S., Suneja, P., 2022. Biogenic synthesis of zinc nanoparticles, their applications, and toxicity prospects. *Frontiers in Microbiology* 13(1), 824427.
- Saravanan, A., Kumar, P.S., Karishma, S., Vo, D.V., Jeevanantham, S., Yaashikaa, P.R., George, C.S., 2021, A review on biosynthesis of metal nanoparticles and its environmental applications. *Chemosphere* 264, 128580.
- Shakiba, S., Astete, C.E., Paudel, S., Sabliov, C.M., Rodrigues, D.F., Louie, S.M., 2020. Emerging investigator series: polymeric nanocarriers for agricultural applications: synthesis, characterization, and environmental and biological interactions. *Environmental Science: Nano* 7(1), 37–67.